ISH Journal of Hydraulic Engineering

ISSN: (Print) (Online) Journal homepage: www.tandfonline.com/journals/tish20

Hydraulics-based pipe leak detection revisited and experimentally verified

S.K. Mishra, Nawaraj Pokhrel, J. Pallavi, Chhavi Raj Jaishi, B.K. Aashish, Abel W. Zena, Andom Y. Ghenzebu & Akhilesh Verma

To cite this article: S.K. Mishra, Nawaraj Pokhrel, J. Pallavi, Chhavi Raj Jaishi, B.K. Aashish, Abel W. Zena, Andom Y. Ghenzebu & Akhilesh Verma (05 Nov 2024): Hydraulics-based pipe leak detection revisited and experimentally verified, ISH Journal of Hydraulic Engineering, DOI: 10.1080/09715010.2024.2418590

To link to this article: https://doi.org/10.1080/09715010.2024.2418590

Published online: 05 Nov 2024.

ISH JOURNAL OF HYDRAULIC ENGINEERING
https://doi.org/10.1080/09715010.2024.2418590

Hydraulics-based pipe leak detection revisited and experimentally verified

S.K. Mishra, Nawaraj Pokhrel, J. Pallavi, Chhavi Raj Jaishi, B.K. Aashish, Abel W. Zena, Andom Y. Ghenzebu and Akhilesh Verma

Department of WRD&M, Indian Institute of Technology Roorkee, Roorkee, UK

ABSTRACT

Leak detection is an integral component of pipelines that often fails due to one or the other reason and leads to several issues of serious concern requiring immediate attention. This paper revisits a technique based on hydraulic principles of flow of water through pipes and verifies it experimentally for its applicability using reasonably large set of data derived experimentally for various pipes of different materials and diameters, pipe flows, and leak discharges/locations. The study finds that the available hydraulic equation for leak localization is valid only for long pipes, not for short pipes experiencing significant impact of leak-generated negative waves on inlet and outlet pressures, too sensitive to localization. The proposed new (more elaborate) equation not only works well for both short and long pipes but also enables a consistent description of the effects of pipe materials, diameters, pipe flows, and leakages and their sensitivity to localization. In an attempt to further support the study results, the acoustics-based measurements were also analyzed for describing the level of leakage in pipes with increasing decibel magnitude, and the results were found to be not only cogent but also consistent in describing the impacts of pipe materials/sizes and leak locations on noise level.

ARTICLE HISTORY
Received 17 April 2024
Accepted 15 October 2024

KEYWORDS
Bernoulli equation; flow through pipes; hydraulics of pipe flow; pipe burst or leak; water leakage

1. Introduction

Recent years have witnessed extensive use of pipelines and pipe networks to transport and distribute fluids like water (Cassa et al. 2010; Adedeji et al. 2017), natural gas (Adegboye et al. 2019a,b; Akinsete and Oshingbesan 2019), oil (Adegboye et al. 2019a,b; Adegboye et al. 2022; De Sousa and Romero 2017), and so on and it is evolving rapidly (Fu and Chen 2024). Pressurized pipe networks may leak or burst due to many reasons, like ageing, corrosion, temperature, high pressure, poor material, poor construction quality, improper operation and maintenance, damage to property and livestock and environmental extremities (Cheng et al. 2018; Abdulshaheed et al. 2018). Leaky pipes may cause not only significant loss of material transported but also leads to social, environmental, and economical hazard (Kang and Lansey 2014; Colombo and Karney 2002; El-Zahab). Therefore, a leak detection system should be able to detect both leakages and their locations for quick maintenance and restoration.

Since the growing population and huge water demand worldwide necessitate the efficient operation of water distribution networks (Romero-Ben et al. 2022; Ali et al. 2022,b), it is crucial not only to improve the reliability of leak detection methods (Lopezlena and Sadovnychiy 2019; Li et al. 2022) but also to monitor the networks continuously. There exist a number of pipeline leakage detection approaches available in literature (Zaman et al. 2020) as enumerated below.

In pipelines, optical fibre pressure sensors can be paired with impulse response function (IRF) for detecting leaks effectively (Zeng et al. 2020). Pan et al. (2023) found the exchange of energy (Lin et al. 2019) occurring in leaking pipelines. Using a modified reconstructive method of characteristics, Kumar and Mohapatra (2022) improved the transient analysis for detecting effectively the partial blocks in both elastic and polymer pipelines. Juliano et al. (2013) used microphones and acoustic sensors for leak detection in a metal pipeline buried in sandy soil.

Specific to water pipelines buried underneath roadways in municipal cities are not only difficult to repair for leaks but also sometimes too difficult to detect or locate them. Hadji et al. (2022) proposed a method for small and multiple (Li et al. 2022; Wang et al. 2022) leakages in such pipelines. Du et al. (2020, 2023) studied the damped fluid transients generated due to the burst or unsteady friction using Fourier analysis and found the transients caused due to branches and loops to be non-distinguishable from those due to bursts. Sophocleous et al. (2019) employed search-space reduction method and suggested data-driven machine learning models to be easily modifiable and most economical alternative (Basnet et al. 2023). To identify small leakages in tap water distribution pipes, the distributed temperature sensing method based on Raman scattering is also used (Wang et al. 2022). Steffelbauer et al. (2022) proposed a method to detect simultaneously multiple leaks in such a network and Jaumouillé et al. (2009) derived a hydraulic equation for the same using Navier-Stokes equations considering leakage – pressure relationship.

Adegboye et al. (2019a,b) classified the methods available in literature as exterior and interior methods. Kammoun et al. (2022) compared various algorithms for performance. Hinderdael et al. (2020) proposed the use of leak-generated negative pressure waves (more prominent in short pipes) in

CONTACT S.K. Mishra s.mishra@wr.iitr.ac.in

(even small) leak detection. Kang and Lansey (2014) experimentally simulated the hydraulic responses to leak detection in a water distribution network and Abdulshaheed et al. (2018) identified the pressure component to rely on pipe material and crack geometry. Notably, hole leaks are common in metallic pipes, and crack leaks in asbestos cement and Polyvinyl Chloride (PVC) pipes. Due to lower leak exponent coefficient, the former exhibits lesser leak discharges than does the latter. Ferrante (2012) investigated experimentally the leak head-discharge relationships in steel and polyethylene pipes.

Cheng et al. (2018) proposed a hydraulic equation assuming leak discharge magnitude to be negligible compared to pipe flow and it is valid for long-pipes only. In this paper, an attempt has been made to further investigate its validity for short pipes and modify it for varying pipe flows and leak discharges using a reasonably large set of data derived from an experimental setup installed in two phases at the demonstration farm of Indian Institute of Technology Roorkee (India) employing Mild Steel (MS), PVC, and High-density Polyethylene (HDPE) pipes of 2” (= 50.8 mm), 3” (= 76.2 mm), and 4” (= 101.6 mm) diameters, each of 230 m in the first and 75 m length in the second phases. With the same experimental setup, an acoustic-based study for assessment of leakage was also conducted as it is one of the simplest and most useful methods of leak detection (Kousiopoulos and Nikolaidis 2022; Fan et al. 2022; Abed et al. 2023; Chatzigeorgiou et al. 2010; Chew et al. 2023; Bakhtawar and Zayed 2021).

2. Methodology

2.1. Existing Cheng et al. (2018) method

Cheng et al. (2018) proposed the following equation for localization of leakage or burst in long-distance water pipelines using hydraulic principles:

$$X = \frac{(P_1' - P_2') - (P_1 - P_2)}{S((Q_2 + \Delta Q)^2 - Q_2^2)} \tag{1}$$

where X = leakage distance from inlet pressure point (m); ΔQ and Q_2 = leakage and outflow discharges, respectively (m^3); Q_1 = inflow discharge (m^3) = Q_2+ΔQ; P_1 and P_2 = inlet and outlet pressures at normal flow conditions, respectively (N/m^2); P_1’ and P_2’ = inlet and outlet pressures after leakage, respectively (N/m^2); *S* = specific pipe resistance derived from Darcy-Weisbach head loss (m) (h_f) equation expressed as: $h_f = SLQ^2$; S = $f/12.11d^5$; L = pipe length between inlet and outlet pressure gauges (m); Q = Q_1; d = diameter of pipe (m); and f is the friction factor (non-dimensional). Equation 1 inheres all the assumptions of Bernoulli equation, is applicable for straight and horizontal pipes, neglects velocity head difference and all minor losses (entry, exit, and bend), is applicable for long distance pipelines having large diameter carrying very high discharge compared to the magnitude of leak discharge.

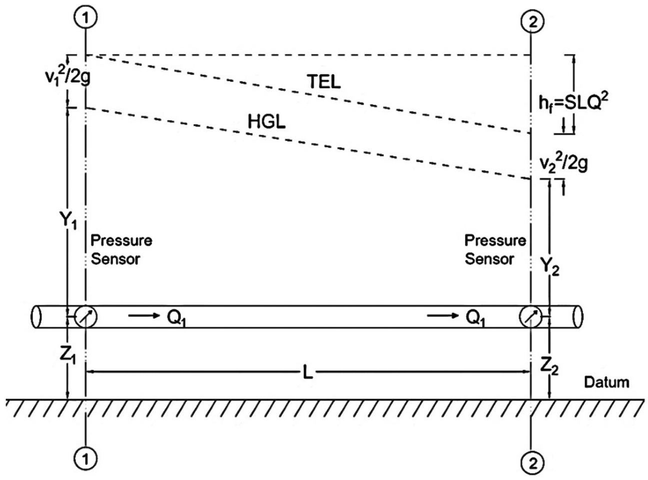

Figure 1(a). Water pipe flow without leakage.

2.2. Proposed methodology for both short and long pipes

Equation 1 holds for leak localization in long-distance pipelines experiencing negligible leakage discharge compared to pipe discharge (i.e. ΔQ << Q_1) and assuming hydraulic grade line to vary linearly with distance of water travel. It is therefore in order to propose a new equation also valid for short pipes using the same hydraulic principles, i.e. based on the universal law of mass and energy conservation, considering all the variables neglected in the development of Equation 1.

2.2.1. Equation for no-leak condition

The law of energy conservation (i.e. Bernoulli equation) between two sections 1–1 and 2–2 Figure 1(a) can be written as:

$$\frac{P_1}{\gamma} + Z_1 + \frac{V_1^2}{2g} = \frac{P_2}{\gamma} + Z_2 + \frac{V_2^2}{2g} + h_f \tag{2}$$

where $\frac{P_1}{\gamma}$ (= Y_1) and $\frac{P_2}{\gamma}$ (= Y_2) are inlet and outlet pressure heads in meter at sections 1–1 and 2–2, respectively; P_1 and P_2 are pressures at sections 1–1 and 2–2, respectively, in N/m^2; Z_1 and Z_2 are datum heads at sections 1–1 and 2–2, respectively, in m; V_1 and V_2 are velocities at sections 1–1 and 2–2, respectively, in m/s; γ is the specific weight = 9810 N/m^3 for water; and g is the acceleration due to gravity = 9.81 m/s^2 h_f is the Darcy-Weisbach friction loss in *m* = $fLV^2/2gd = SLQ_1^2$; S = specific pipe resistance = $f/12.11d^5$; L is the length of pipe between sections 1 and 2 in m; d is the diameter of pipe in m; Q_1 is the inlet discharge in no leak condition in m^3/s; f is the friction factor (non-dimensional). For no-leak condition, V_1 and V_2 (=V_1) are average velocities at sections 1 and 2, respectively Figure 1(a) and for levelled and horizontal pipeline, Z_1 = Z_2. Thus,

$$Y_1 - Y_2 = SLQ_1^2 \tag{3}$$

In Figure 1(a), which describes the flow hydraulics through a pipeline under no-leak condition, HGL is the hydraulic gradient line, TEL is the total energy line, and GL is the ground level.

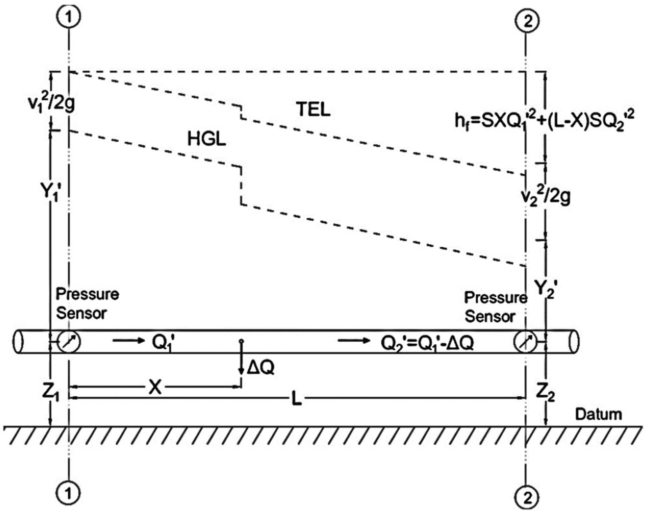

Figure 1(b). Pipe flow with leakage.

2.3. Equation for leakage condition

Applying Bernoulli equation for leakage condition as in Figure 1(b) leads to

$$\frac{P_1'}{\gamma}-\frac{P_2'}{\gamma}+\frac{V_1'^2}{2g}-\frac{V_2'^2}{2g}=SXQ_1'^2+S(L-X)Q_2'^2 \tag{4}$$

Or,

$$Y_1'-Y_2'=SXQ_1'^2+S(L-X)Q_2'^2-0.0826*\left(\frac{Q_1'^2-(Q_1'-\Delta Q)^2}{d^4}\right) \tag{5}$$

Subtracting Equation 3 from Equation 5 and simplifying, the location of leakage (X) can be derived as:

$$X=\frac{(Y_1'-Y_2')-(Y_1-Y_2)+SL\left(Q_1^2-(Q_1'-\Delta Q)^2\right)+0.0826*\left(\frac{Q_1'^2-(Q_1'-\Delta Q)^2}{d^4}\right)}{S(Q_1'^2-(Q_1'-\Delta Q)^2} \tag{6}$$

where X is the distance between the inlet pressure gauge and the leakage point in m; $Y_1'(=\frac{P_1'}{\gamma})$ and $Y_2'(=\frac{P_2'}{\gamma})$ are the inlet and outlet pressure heads after leakage, respectively, in m; P'$_1$ and P'$_2$ are pressures at sections 1–1 and 2–2, respectively, in N/m^2; Q_1' and Q_2' are the inflow and outflow discharges, respectively, in m^3/s; and ΔQ = leakage discharge = Q_1' - Q_2'. Equation 6 can be used for leak localization in pipeline network by analyzing the observed data and is valid for even short pipes, for it accounts for the variation in pressures and discharge both before and after the leak occurrences.

3. Experimental setup and data collection

3.1. Experimental setup

Total nine MS, PVC, and HDPE (approximately 230 m long) pipes of 2", 3", and 4" diameters (Table 1 & 2) were laid side by side on masonry walls as shown in Figures 2(a,b,c). Using the gate valve in 6-inch (= 152.4 mm) diameter inlet pipe, the water was supplied to all 9 pipes. Water in each pipe was further regulated using ball valves. Two flowmeters were used for each pipe, one near inlet, and the other near outlet. Leakage points were artificially introduced at points with knobs to regulate leakages (as shown in Table 1) and their water was collected in bucket and it was measured using a measuring jar. A pressure gauge was installed just downstream of every leak point, one after the flowmeter near inlet, and the other near outlet to measure pressure variations occurring in pipes before and after the occurrence of leakage.

3.2. Data collection

For determination of the distance of leak point X from the inlet point (i.e. the location of pressure gauge), Equation 6 was used. It required the measurements of inflow discharge Q_1, outflow discharge Q_2, Inlet pressures P_1 and P_1', and Outlet Pressures P_2 and P_2', where P_1 and P_2 are pressures before leakage, and P_1'& P_2' after leakage. The leakage discharge ΔQ was measured for all 9 pipes for different pipe flows regulated via valves for 100%, 50%, and 25% (approx.) pipe-valve openings.

Table 1. Details of different pipe dimensions and leak locations used in the two sets of experiments. 1 inch = 25.4 mm.

			Pipe length (between inlet and outlet pressure gauges) (m)		Leak location from inlet pressure gauge (m) in three experimental setups					No. of observations	
					1st Setup		2nd Setup		3rd Setup		
S.N.	Pipe material	Pipe size (inch)	With Bend	Without Bend	With Bend	Without Bend	With Bend	Without Bend	With Bend	With Bend	Without Bend
1	MS	2	225	65	22	14	51	47	174	36	24
		3	228	65	22	13	51	47	177	36	24
		4	234	64.5	22	14	51	47	182	36	24
2	PVC	2	226	64	21	13	51	47	175	36	24
		3	229	64	21	13	51	47	177	36	24
		4	231	67	21	17	51	49	179	36	24
3	HDPE	2	232	63	55	13	178	44	222	36	24
		3	226	63	26	13	55	44	175	36	24
		4	230	63	22	13	51	42	179	36	24
Total										324	216

Figure 2(a). Photograph of the experimental setup at Roorkee (India).

Similarly, leakage was allowed at two locations and its magnitude was regulated for 100%, 50%, 25% (approx.) leak-knob openings, and no leak condition as well. Table 2 shows both absolute inflow and leak discharge values observed in an experimental setup, each repeated three times for averaging. In this fashion, in the first phase of experimentation, 36 measurements were taken for one pipeline, and thus, a total of 324 observations for all 9 pipelines, as shown in Figure 2(b) and Table 1. The *-marked values in Table 2 indicate the experimental observations to have been excluded from the analysis as the pressurized flow did not exist at the pipe outlet in these experimental runs. Similar to Phase 1, 216 observations (Figure 2(c) and Table 1 & 2) were taken in the second phase for verification. Besides, water temperature was recorded using thermometer for change in water viscosity, if any. The labor-intensive experimentation work required several skilled and unskilled human resource for measurements and recordings.

4. Analysis and discussion of results

In the present study, there are three terms worth explaining. 1. 'Total length of pipe' is the pipe length actually laid in field as a part of experimental setup, i.e. of the order of 230 m. 2. 'Longer Pipe length' and 'Shorter Pipe length' designate respectively the comparative lengths of pipes between the two pressure gauges (installed) in two experimental setups. 3. 'Hydraulically Long Pipe' and 'Hydraulically Short Pipe' denote respectively the relative hydraulic conditions when upstream pressure is not much impacted or much impacted, respectively, by the negative wave produced due to leak opening in two experimental setups. Furthermore, only a single leak is considered in an experimental run and, before analysis, the data was processed for consistency.

4.1. Data processing

To check the validity and consistency of observations of the first phase of experimentation Figure 2(b), the friction factor (f) was derived from Moody diagram, and head computed from Darcy-Weisbach equation:

$$h_f = fLV^2/2gd \tag{7}$$

It was found that the derived head loss values were higher than the corresponding total pressure drops observed between inlets and outlets (both representing the locations of pressure gauges) in most sets of observations. To check this data for consistency, another set of similar 216 observations was derived in the second phase of experimentation for straight but different (approximately 75 m) long pipes as shown in Figure 2(c) for, as an example, PVC pipe. The inlet flowmeter and pressure gauge were installed at a distance of 10 m from the flow regulating valve of the respective pipeline to avoid the valve effect. In this new pipeline, two leaks were introduced at 14 m and 44 m approximately from the inlet pressure gauge. In this fashion, 24 measurements were taken for one pipeline. (i.e. 216 for 9 pipe lines of three materials and three sizes)

The frictional losses calculated using 'f' (from Moody diagram) were higher than the corresponding total pressure drops observed also for new set of observations. It led to re-

Table 2. Inflow and leak discharges for full (or 100%) pipe opening and corresponding leak discharges. 1 inch = 25.4 mm.

			Inflow (m^3/s) for full (or 100%) inlet pipe opening in three experimental setups					Leak discharge (m^3/s) for full (100%) opening of nozzle				
			1st Setup		2nd Setup		3rd Setup	1st Setup		2nd Setup		3rd Setup
S. N.	Pipe material	Pipe size (in)	With Bend	Without Bend	With Bend	Without Bend	With Bend	With Bend	Without Bend	With Bend	Without Bend	With Bend
1	MS	2	0.0021777	0.00229160	0.0021666	0.0022583	0.0021777	0.0002388	0.00059410	0.00011110	0.0003495	0.00019160
		3	0.0061722	0.00618880	0.0061888	0.0062611	0.0064500	0.0002277	0.00082140	0.00021660	0.00053996	0.00037770
		4	*	0.01052638	*	0.0109583	*	*	0.00091930	*	0.0009286	*
2	PVC	2	0.0023083	0.00223981	0.0020611	0.0021361	0.0023056	0.0002110	0.00078351	0.00011110	0.00049149	0.00009720
		3	0.0064833	0.00563880	0.0063805	0.0054166	0.0061472	0.0002944	0.00027477	0.00011388	0.00048148	0.00019400
		4	*	0.01021527	*	0.0096986	*	*	0.00063440	*	0.00064060	*
3	HDPE	2	0.0024944	0.00229166	0.0025666	0.0022694	0.0025472	0.0002777	0.00050506	0.00044720	0.00064676	0.00027770
		3	0.0052500	0.00497770	0.0050638	0.0049944	0.0052500	0.0002499	0.00026108	0.00025000	0.00057490	0.00036388
		4	*	0.00841100	*	0.0087888	*	*	0.00041865	*	0.00078477	*

*Data could not be recorded in 4″ pipe (with bend) experiment for low pressure reasons at the pipe outlet.

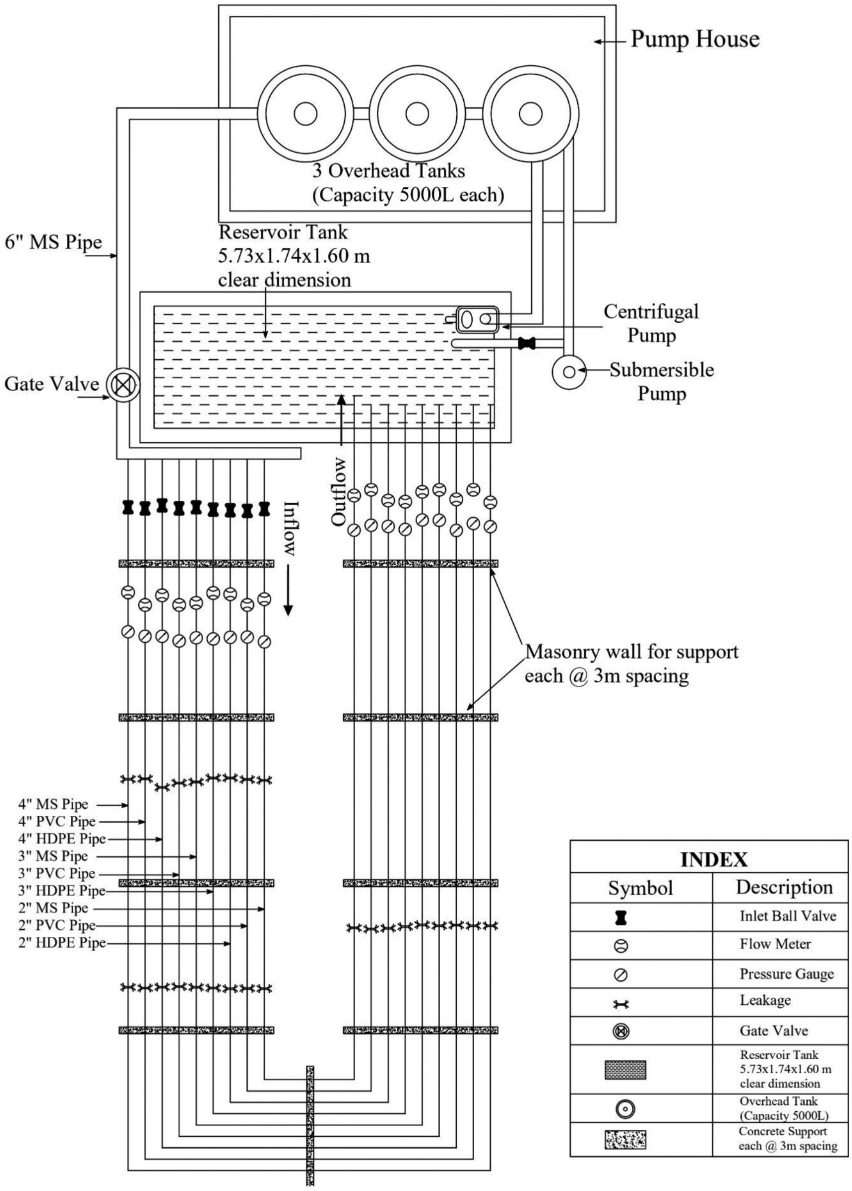

Figure 2(b). Detailed layout (plan) of pipe network at the experimental site.

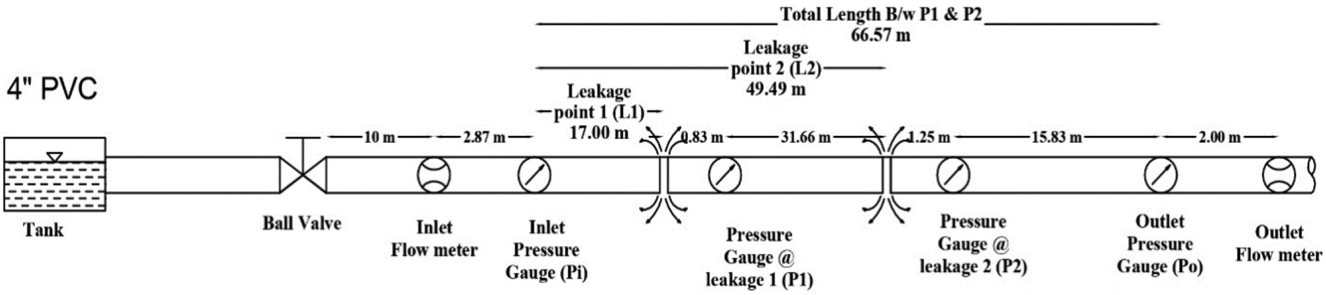

Figure 2(c). Pipeline layout of 4″ PVC (as an example) pipe with leakage.

checking of f-values derived from Moody diagram for different materials. In this diagram, since 'f' for a particular pipe exhibits insignificant variation at extremely high (~10^6) Reynolds numbers, it was rederived using the observed data for all material pipes for no-leak condition from Equation 7, and the resulting values are shown in Figures 3 (a–c) for MS, PVC, and HDPE pipes, respectively. It can be seen that the values of 'f' derived from the observed data were generally lower than those derived from Moody diagram. To refine the observations, the small deviations in these f-values Figures 3(a–c) were averaged to arrive at a reasonable f-value for a pipe, as shown in Table 3, and it allowed processing of the observed discharge data for further use in analysis.

4.2. Simulation of leak locations

In the first experimental setup, i.e. with bend (Figure 2(b) & Table 1) for 4" pipes of all materials, as also mentioned earlier, the flow in pipes at the outlet acted as an open

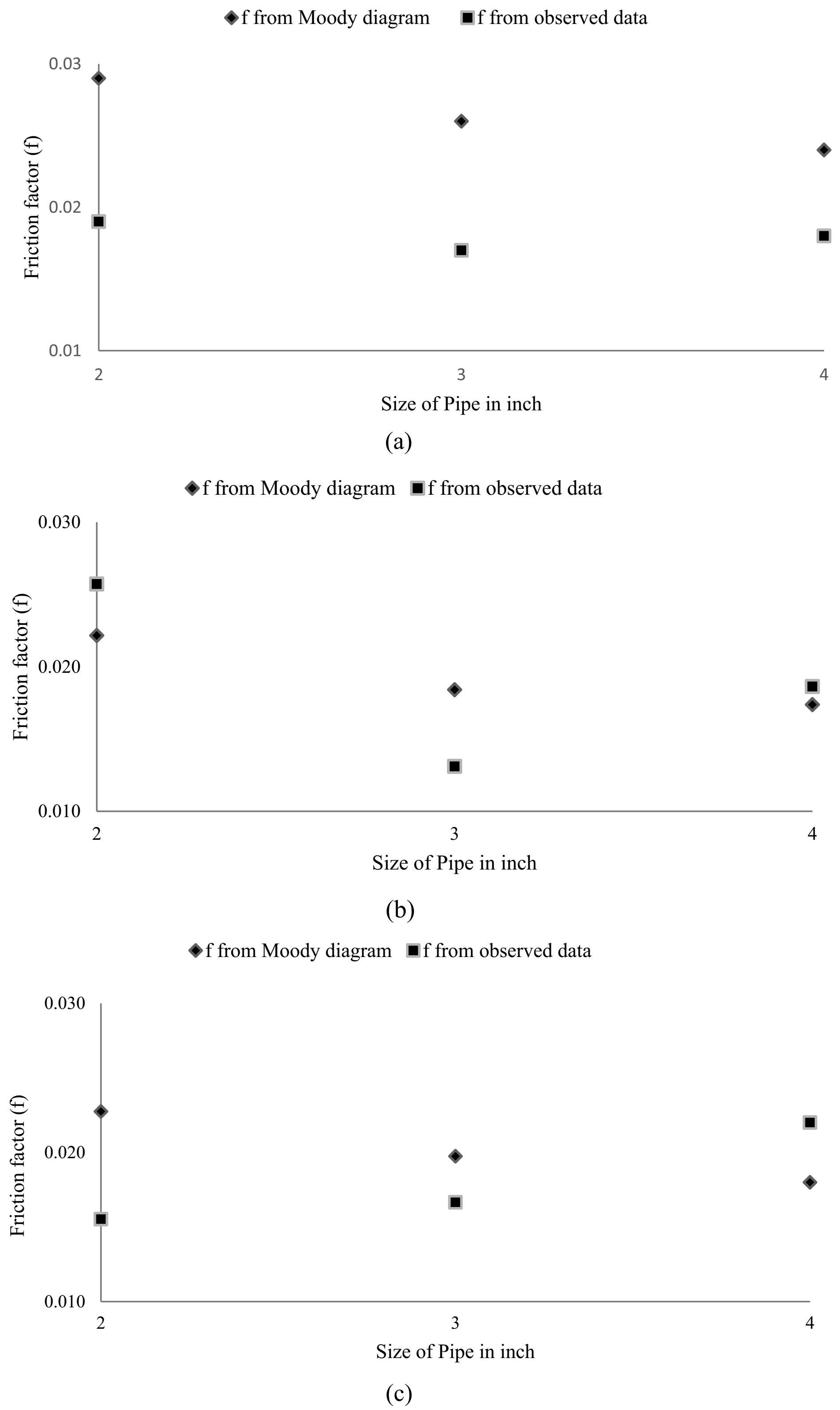

Figure 3. Friction factor (f) values derived from Moody diagram and Darcy-Weisbach equation for (a) MS, (b) PVC, and (c) HDPE pipes.

channel flow because of insufficient pressure existing there, and therefore, a booster pump was installed for raising the pressure but it resulted in high fluctuations and did not allow accurate measurements of pressure, quite sensitive to leak localization. Therefore, the data of the first experimental setup for 4” pipes of all materials was excluded from further analysis.

Equation 6 was used for leak localization for both experimental datasets (Table 1 & 2) derived for with (Figure 2(b)) and without (Figure 2(c)) bend in pipes for both short (less than 55 m long) and long (of the order of 175 m or longer) pipes and the resulting values are compared with the observed or measured ones in Figure 4. In this figure, four sets of observations can be clearly seen. The first two sets, i.e. 1st and 2nd (from left to right) are for short pipes (Table 1) and these correspond to leak locations near and away from the inlet, respectively. The other two sets similarly correspond to long pipes for 3rd setup shown in Table 1. It can be seen from Figure 4 that the calculated values deviated from the observed ones by ± 12.6%, which is tolerable

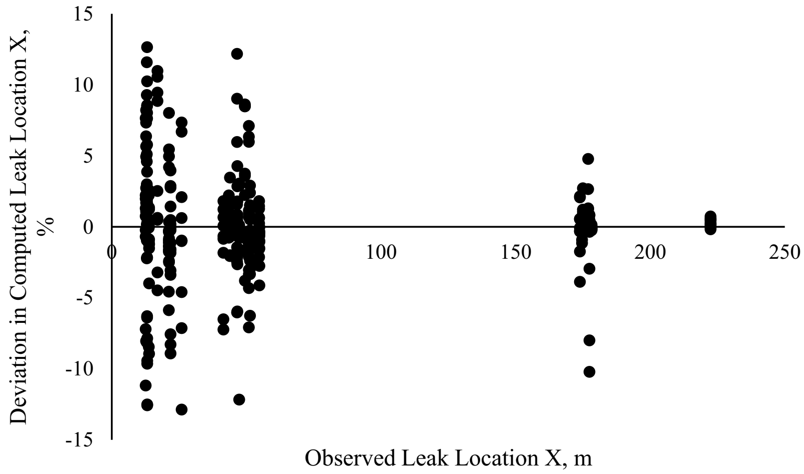

Figure 4. Percent deviation of computed (equation 4) leak locations from the observed ones.

Table 3. Values of friction factor (f) derived for various pipe materials and sizes. 1 inch = 25.4 mm.

		Pipe size		
S.No.	Material type	2″	3″	4″
1	MS	0.019	0.017	0.018
2	PVC	0.022	0.013	0.017
3	HDPE	0.016	0.017	0.018

Table 4. Percent deviation of computed leak location from the observed one in each leak position.

S. No.	Leak location (m) from inlet pressure gauge	% deviation in leak position (range)		
Short pipes (1st and 2nd Experimental Setups) (Table 1 & 2)				
1	13	0	to	±12.6
2	14	0	to	±9
3	17	0	to	±11
4	21	0	to	±8
5	22	0	to	±9
6	26	0	to	±12.6
7	42	0	to	±7
8	44	0	to	±2
9	47	0	to	±12
10	49	0	to	±9
11	51	0	to	±7
12	55	0	to	±4
Long Pipes (1st and 2nd Experimental Setups) (Table 1 & 2)				
13	174	0	to	±4
14	175	0	to	±1
15	177	0	to	±10
16	178	0	to	±0
17	222	0	to	±1

considering the sensitivity and accuracy of data observed under the environment of fluctuating pressure readings, and neglecting entry and exit, bend and other losses occurring due to obstructions created by fittings in a pipeline. It can be inferred from Figure 4 that the deviation in leak location is generally (in majority of cases) higher when the leaks are located near the inlet pressure gauge in case of both short and long pipes, largely due to higher effect of leak-generated negative waves (Hinderdael et al. 2020), and vice versa. When the leak is located after the pipe bend (in the direction of flow), the effect of negative pressure wave on inlet pressure measurement is greatly reduced, leading to negligible deviation from observed leak locations. Table 4 shows for both short and long pipes (as described above) the numerical values of the lumped range of percent deviation of the same calculated leak locations from the observed ones in all four sets. These values also lead to drawing generally similar inference as drawn from Figure 4.

4.3. Impact of negative wave on inlet pressure

The above inference of Figure 4 can be further strengthened using the same concept of leak-generated negative wave (Hinderdael et al. 2020) on inlet pressure measurements that are quite sensitive to leak localization. This concept is quite similar to that (Kocaman et al. 2021) of the negative wave propagating upstream during emptying of reservoir/ channel during dam/channel break, respectively, which

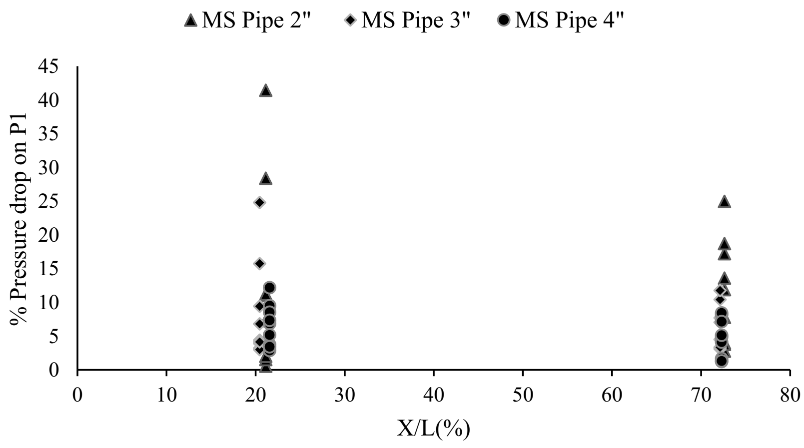

Figure 5. Effect of negative wave on inlet pressure due to leakage location.

affects the heads upstream. Figure 5 shows the effect of negative wave on inlet pressure for all 2", 3", and 4" pipes of all materials for different flow and leak conditions at different leak locations. In this figure, only two leak locations are visible, largely for the reason that the leaks in all cases of pipe flows were placed, as shown in Table 1 & 2, at about 20–25% or 70–75% of the considered pipe length (between two pressure gauges) in an experimental run. It can thus be inferred that, for all types of pipe materials, as the leak distance from inlet point increases, the percent drop in upstream pressure decreases, and vice versa. A similar analysis (not shown) was also carried out for evaluating the impact of leakage rate on the inlet pressure. It was found that as leakage rate increased, the corresponding decrease in inlet pressure also increased linearly and it was in accordance with the expectation as above. The larger the leakage rate, the greater the disturbance created, and the larger the impact on inlet pressure, and vice versa. For the given pipe flow and leak conditions, the impact on inlet pressure in flow through HDPE pipe was less than that in PVC pipe and further less than that in MS pipe, implying that the material of pipe affected the propagation characteristics of negative waves. It was higher in smaller diameter pipes, and vice versa. For all pipe sizes and materials, it was more pronounced if X/L (where X is the leak location from inlet pressure gauge and L is the pipe length between the two pressure gauges) was less, and vice-versa.

Similar to the above, a plot was drawn between (X/L)*(ΔQ/Q1') (%) and decrease in inlet pressure (%) (= (P1-P1')*100/P1) and it is shown in Figure 6 for 4" pipes of all materials. It can be seen that the latter increases as the former increases, implying that the impact of leak rate, i.e. ΔQ/Q1', is much more pronounced than the leak location, i.e. X/L. In addition, different materials impact differently, for example, for a given X/L and ΔQ/Q1' the impact of MS pipe on decrease in inlet pressure is most pronounced, and that of HDPE, the least. PVC impacts intermediately. It is possible to account for the impact of pipe material, pipe size, inflow discharge magnitude quantitatively, as follows.

$$\Delta Y_1(\%) = -2.66 + 40.24(\Delta Q/Q_1')^{0.54} + 10\left(\frac{\varepsilon}{d}\right)^5 + 13.71(Q_i/Q_{100})^{-0.36} - 16.24(X/L)^{0.14}, R2 = 0.575 \tag{8}$$

where $\Delta Y_1(\%)$ is the percent reduction in inlet pressure = $(Y_1 - Y_1')/Y_1 * 100$; both Y_1 and Y_1' are pressure heads (m). The constant, coefficients, and exponents are derived using

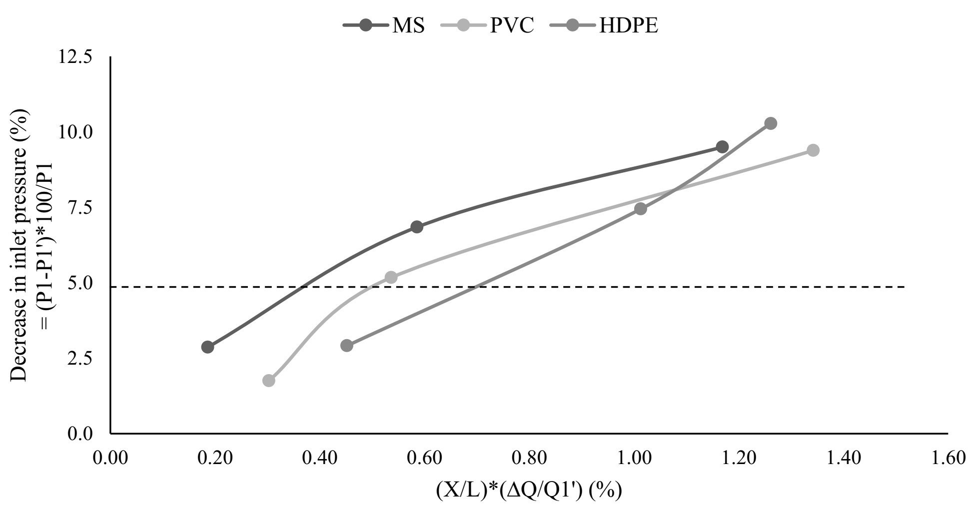

Figure 6. Percent decrease in inlet pressure for 4" pipes of all materials.

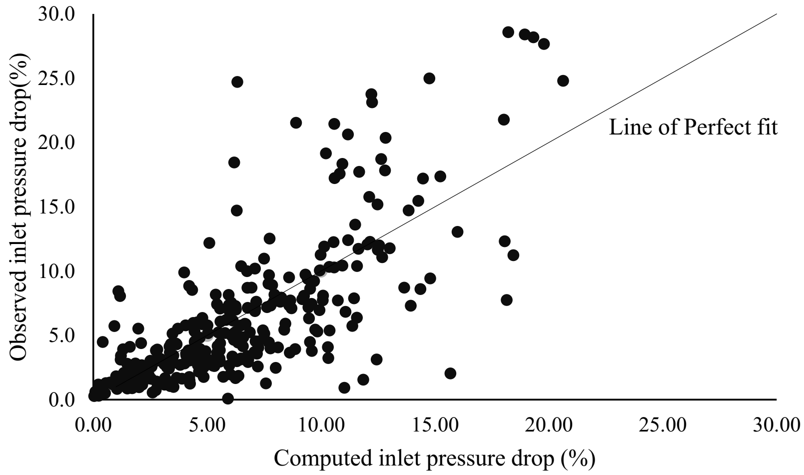

Figure 7. Observed versus computed inlet pressure drop (%).

complete dataset and employing the MS Excel Solver tool by minimizing the root mean square error (RMSE); ε is the roughness coefficient ($= 0.15 \times 10^{-3}$m, 0.0025×10^{-3}m, and 0.0025×10^{-3}m for MS, PVC and HDPE pipes, respectively); Q_i is the main pipe (actual) pipe discharge (m^3/s) and Q_{100} is the discharge (m^3/s) when pipe is opened full. Equation 7 has been derived with RMSE = 3.96 m (coefficient of determination, $R^2 = 0.575$) for the observed $\Delta Y_1(\%)$ values ranging (0.276 m, 28.6 m). This equation suggests that the pipe flow and leakage magnitudes and the material type impact ΔY_1 positively whereas leak location impacts negatively, which is consistent with the expectation as also described later. Figure 7 depicts the satisfactory closeness of the computed and observed inlet pressure drops (%) depicted by the line of perfect fit, for which $R^2 = 1.0$.

4.4. Description of hydraulically short and long pipes

From the above negative wave characteristics, it is possible to define a pipe to be hydraulically long or short for a given leakage condition, simply by measurements of the inlet pressure before and after the occurrence of leak, as above. To this end, the quantitative impact of the negative pressure on the inlet pressure can be used (Figure 6) as an indicator. Ideally, the impact of leak-generated negative wave on inlet pressure measurements must be near zero if the pipe is long enough. However, for pragmatic reasons, for a given leak discharge, a pipe of given material can be described to be hydraulically long if the percent decrease in inlet pressure is less than 5% (as shown by dotted line in Figure 6) or any other appropriate lower value. Accordingly, a 4” MS pipe is hydraulically short if the percent value of X/L*ΔQ/Q1’ is less than or equal to 0.38, a 4” PVC pipe is short if this percent value is less than or equal to 0.50, and a 4” HDPE pipe is short if the percent value is less than or equal to 0.70. Similar criteria (not shown here for space reasons) can be derived for varying pipe sizes. Accounting for impacts of all factors as included in Equation 7, a general criterion for 5% error can be given by the following inequality for a pipe to be hydraulically long:

$$40.24(\Delta Q/Q_1')^{0.54} + 10\left(\frac{\varepsilon}{d}\right)^5 + 13.71(Q_i/Q_{100})^{-0.36} - 16.24(X/L)^{0.14} < 7.66 \quad (9)$$

Otherwise, the pipe is hydraulically short.

4.5. Impact of velocity head on leak location

Figure 8 shows the percent deviation in leak location computed using Equation 6 without considering the difference in velocity head. It can be seen that the error in computed leak

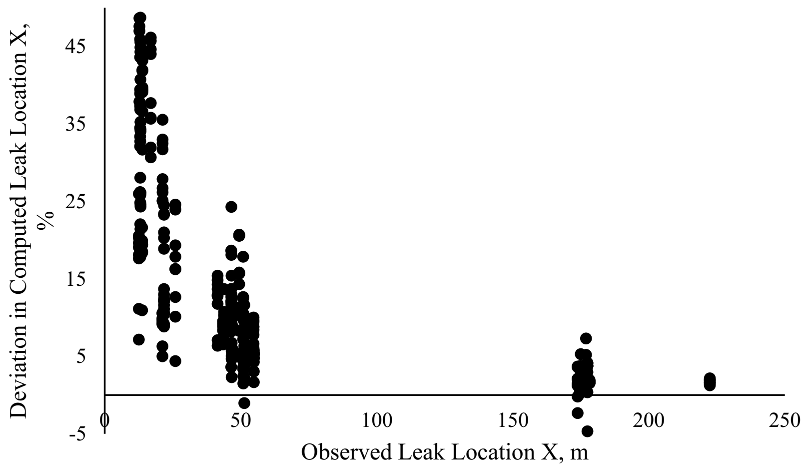

Figure 8. Percent deviation in leak location computed using equation 4 without considering the difference in velocity head.

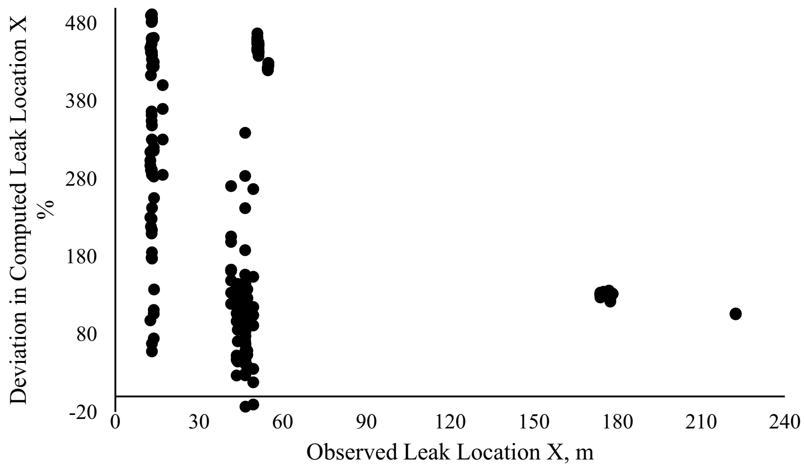

Figure 9. Percent deviation in calculated leak location using equation 1.

location is quite low Figure 4 when velocity head is considered in Equation 6 and it exceeds by 40% when not considered Figure 8. This is an important component of Equation 6 as it accounts for all other losses than pipe length-dependent friction having occurred during pipe flow between sections (1) and (2) and it will be more pronounced than friction in short pipelines, and vice versa. Hence difference in velocity head plays a significant role in leak localization in short pipelines.

4.6. Evaluation of equation (1)

Figure 9 shows the percent deviation in leak location computed using Equation 1. In other words, it evaluates the performance of Equation 1. The larger the deviation, the poorer the performance, and vice versa. It can be seen that the deviation from the observed leak location is very high, even of the order of 500%. In addition, though the leak located after the bend in pipeline impacts the inlet pressure insignificantly, the error estimated is of the order of 100% whereas it is near zero when Equation 6 is used for the leaks located after the bends. Hence, Equation 6 can be used for leak localization in any span of pipelines of any material and diameter or length.

4.7. Effect of material on accuracy of leak localization

Table 3 shows the percent deviation of the computed leak position from the observed one and the overall range is 0–12.6%. A close investigation of the error data (not shown here) revealed that the error in computed and observed leak locations was within the range of 0 to ± 12.6% for MS and HDPE pipes, and it was 0 to ± 11.2 % for PVC pipes in both sets of experiments, i.e. with and without bend for different flow and leak conditions. To evaluate the impact of pipe material on leak localization, the computed leak locations with respect to the observed ones are plotted in Figures 10(a–c) for MS, PVC, HDPE pipes, respectively. In these figures, the dotted line indicates the line of perfect fit, for which $R^2 = 1.0$, implying the fit to be perfect. It can be seen that leak localization from Equation 6 doesn't seem to be much different from one material to other. Though the parameter S in Equation 6 is different for different materials, the sensitivity analysis (shown later) shows that its influence is not much significant in leak localization.

4.8. Effect of pipe diameter on leak localization

Similar to the above description for the effect of pipe material on leak localization, the error data (not shown here) was further investigated and it was found that there was not much significant effect of pipe diameter on leak localization, for the errors in computed and observed leak locations ranged (0, ±12.64 %), (0, ±12.57 %), and (0, ±12.17 %), for 2", 3" and 4" pipes, respectively, and it is shown by the closeness of data points to the line of perfect fit in Figure 11, for different diameters of pipes, pipe flows, and leak discharges in both sets of experiments.

4.9. Sensitivity analysis

For evaluating the sensitivity of different variables used in Equation 6 for leak localization, a sensitivity analysis was carried out for one set of observations and the results are shown in Figure 12. It can be seen that the pressure and pipe discharge are the most sensitive to leak location. Hence, an utmost care be taken while measuring them in field. The degree of sensitivity depends on leak location with respect to the location of inlet pressure gauge. Nearness of the leak point with inlet pressure gauge affects the readings at inlet, and vice-versa for leak located near the outlet pressure gauge. The length, diameter, and friction factor are however not much sensitive.

4.10. Use of leak noise (acoustics) in leak detection

As also stated earlier, to also investigate the workability of the acoustics-based methodology for leak detection, the noise generated during the pipe leak was measured in decibel for different pipes and leak discharges at different locations from the distances of 0.2 m and 0.4 m measured from a pipeline. Figure 13(a) shows the variation of decibels (observed at 0.2 m) with respect to leakage rate for 2" pipe (as an example) with 100% discharge. It can be seen that the minimum value of decibels shows no (or insignificant) leakage and when leakage starts, the decibels increase to reach a critical point and attain a constant value in all sets of observations for all pipes and all pipe and leak discharges. Figure 13(b) shows a similar trend for

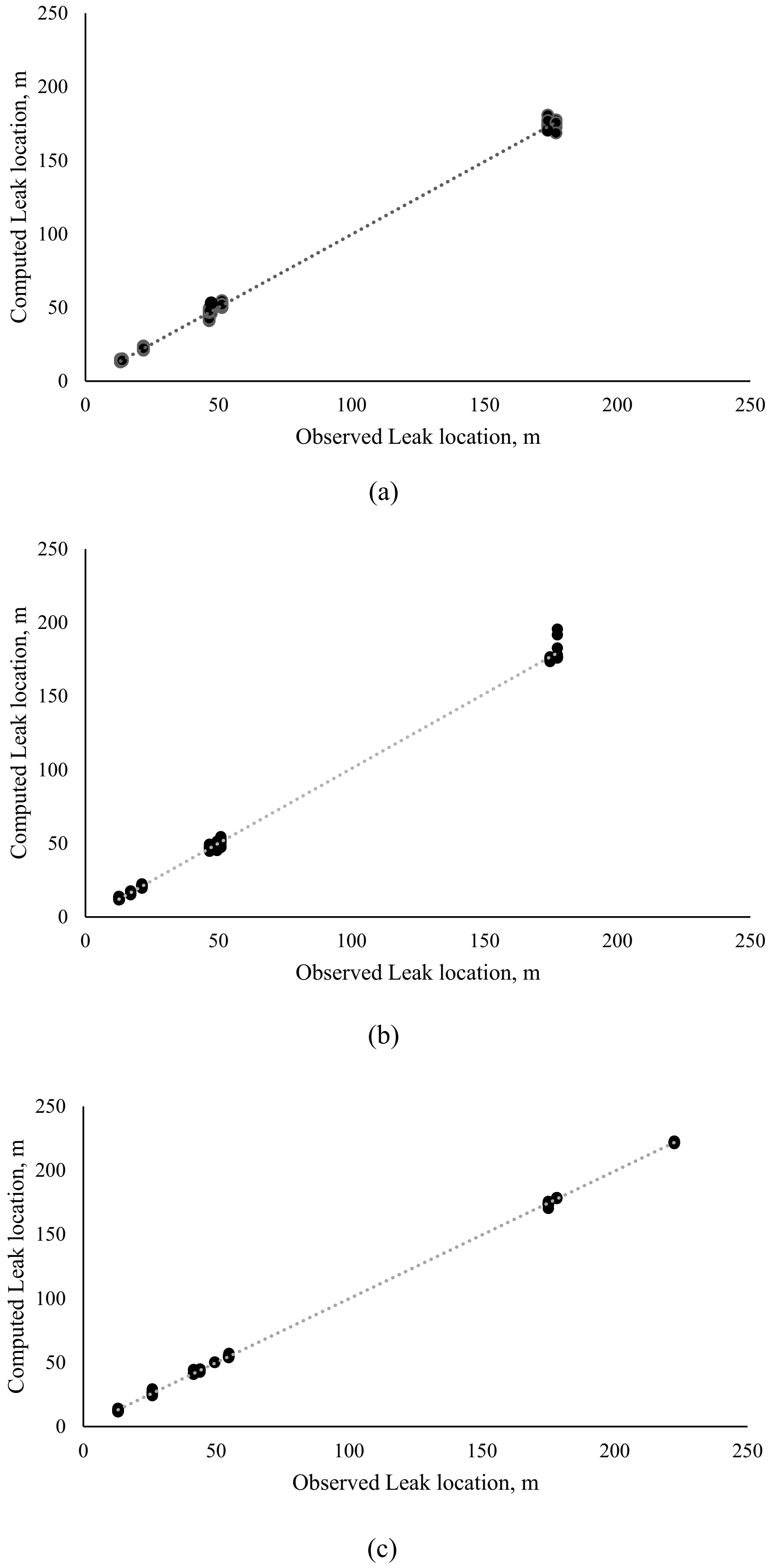

Figure 10. Effect of material on leak localization for (a) MS, (b) PVC, and (c) HDPE pipes.

a distance 0.4 m from pipeline for 2” pipes of all materials. It is further supported in Figure 13(c) showing the effect of leak magnitudes on decibels for MS pipe of different sizes with, as an example, 100% discharge. Interestingly, the trends seen for all pipe sizes are not only consistent but also in line with the general expectation.

5. Limitation of the study

It is in order to also enumerate the major limitations of the study as follows:

(i) The applied methodology is based on the available hydraulic principles, i.e. the Bernoulli equation, and

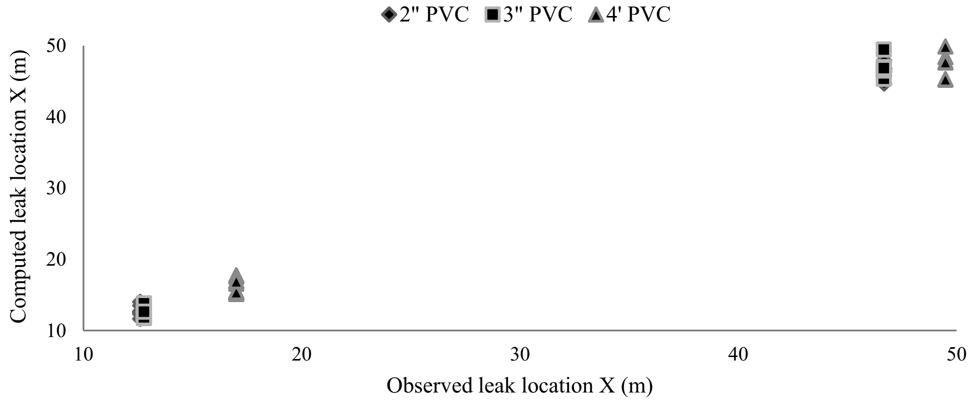

Figure 11. Comparison of computed leak location with observed values for different sizes of pipes.

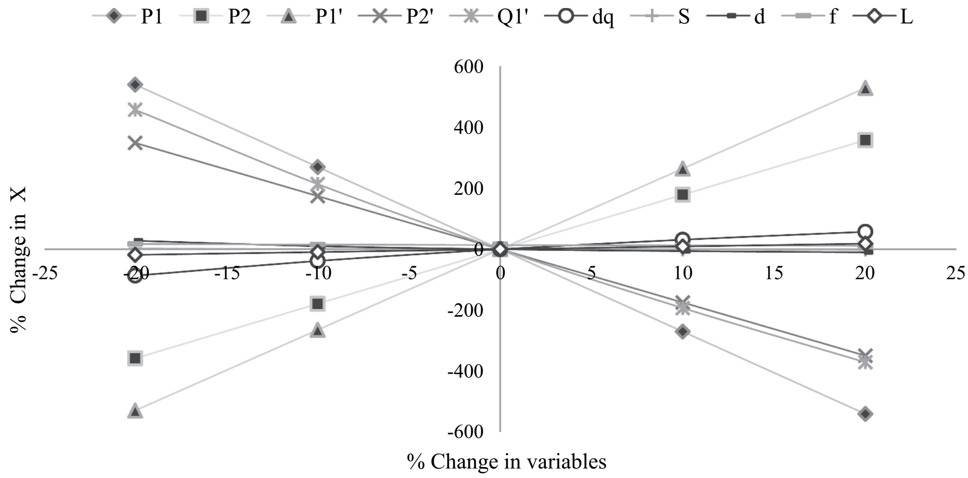

Figure 12. Sensitivity analysis of different variables to leak localization.

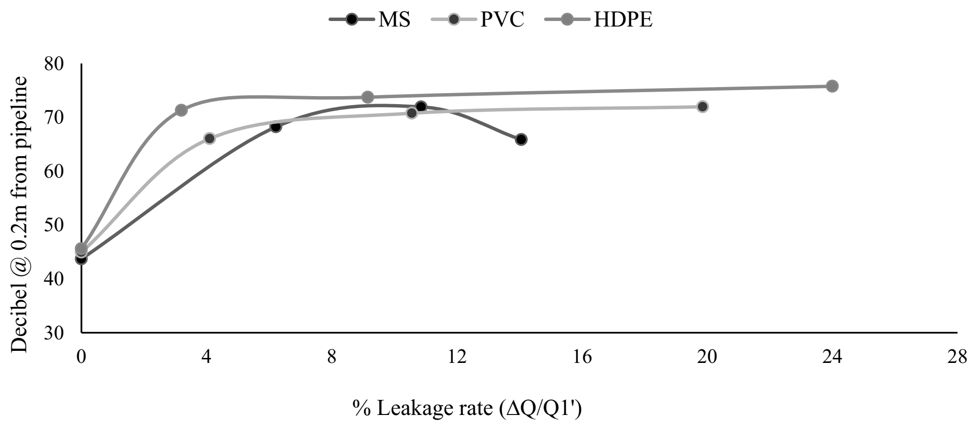

Figure 13(a). Effect of leakage on decibels in 2″ pipes of different materials for 0.2 m distance from pipeline.

therefore, the analysis incorporates all limitations of this equation.

(ii) The experimental setup installed at IIT Roorkee had been a much simplified version of the real networks as it does not consider the real-life complex cross-linkages, bends/transitions, varying pipe sizes/materials/fittings, etc.

(iii) The flow and pressure observations are subject to instrumental as well as human errors.

(iv) The steady flow results are subject to the unavoidable disturbances in water head and flow due to pipe valve openings.

(v) The acoustic data is subject to unavoidable noises of the surroundings.

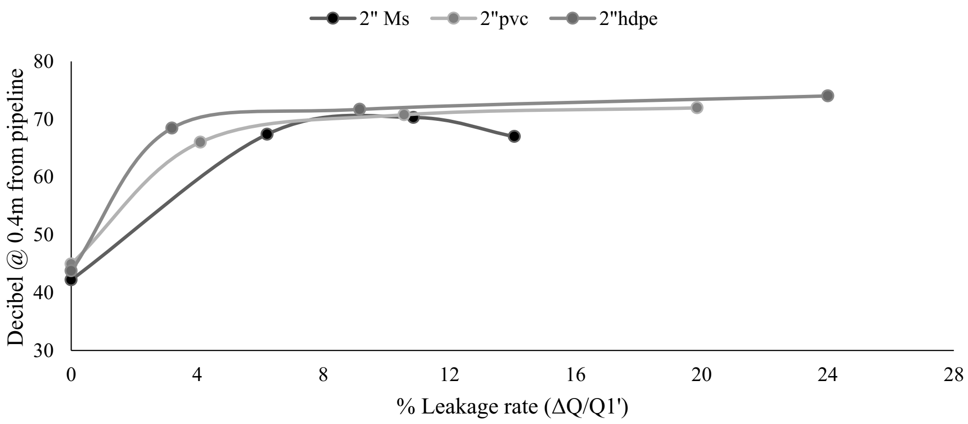

Figure 13(b). Effect of leakage on decibels in 2″ pipes of different materials for 0.4 m distance from pipeline.

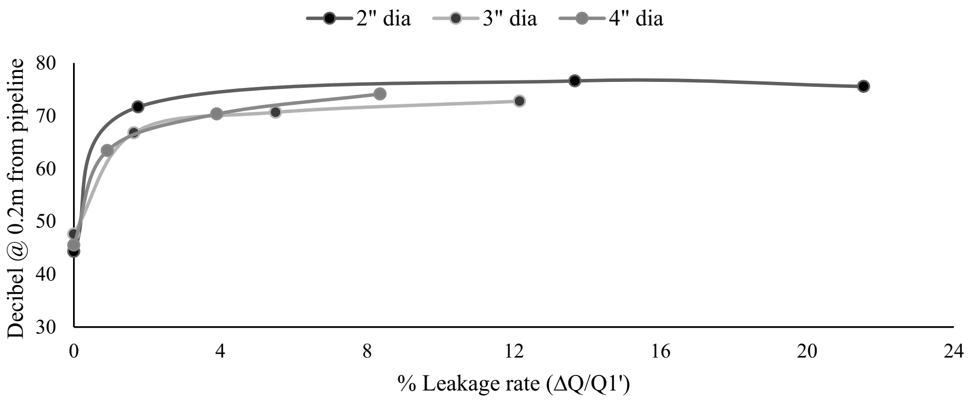

Figure 13(c). Effect of leakage on decibels in MS pipes of different sizes.

(vi) The study also suffers from the scale effect.

Despite the above limitations, the results of the study are quite encouraging and enlightening for future research in this direction.

6. Summary and conclusions

The two sets (with and without bends, i.e. straight) of experiments were conducted for different pipe materials, their diameters, lengths, leak locations at Roorkee (India) for measurements of hydraulic variables, such as inlet and outlet discharges and pressures used for derivation of the magnitudes of leak discharges and leak locations. The following conclusions can be derived from the study:

(i) The available (existing) equation for leak localization is applicable to hydraulically long pipes only, and not for short pipes, and the proposed more elaborate equation is applicable to both types of pipes.
(ii) The above is largely attributed to the ignorance of difference in velocity heads of Bernoulli equation and the assumption of leak discharge to be insignificant compared to the magnitude of pipe discharge.
(iii) The pressure measurements, quite sensitive to leak localization, are affected by the leak-generated negative wave, as expected, more in short pipes than in long pipes.
(iv) The proposed expression (Equation 9) quantifies reasonably well the impact of negative wave on inlet pressure and leads to definition of hydraulically short and long pipes.
(v) The acoustics-based measurements not only consistently describe the level of leakage rate in pipes but also support the inferences drawn in this study.
(vi) Being among a very few experimental studies conducted world-wide, specifically in India, and reported in literature so far, the promising results of the present study may pave a way for future extensive research in this direction.

Acknowledgements

The authors owe to the National Mission on Himalayan Studies, Almora, for sponsoring the R&D project under which the work presented herein was carried out. Secondly, the cooperation of the WRDM Dept. and SRIC, IIT Roorkee is fully acknowledged and appreciated.

Disclosure statement

No potential conflict of interest was reported by the author(s).

Funding

The work was supported by the national mission on himalayan studies almora [GBPNI/NMHS/2020-21/MG/27//].

Data availability statement

Some or all data, models or code that support the findings of this study are available from corresponding author upon reasonable request.

Symbols

HGL	Hydraulic gradient line
TEL	Total energy line
L	Length between inlet and outlet pressure gauge in meter
X	Leakage distance from inlet pressure gauge in meter
P_1	Inlet pressure in no leak condition in N/m^2
P_2	Outlet pressure in no leak condition in N/m^2
P'_1	Inlet pressure at leakage condition in N/m^2
P'_2	Outlet pressure at leakage condition in N/m^2
Q_1	Inlet flow in no leak condition in m^3/s
Q_2	Outlet flow in no leak condition in m^3/s
Q'_1	Inlet flow at leakage condition in m^3/s
Q'_2	Outlet flow at leakage condition in m^3/s
ΔQ	Leakage discharge in m^3/s
Y_1	Inlet pressure head in meter in no leak condition
Y_2	Outlet pressure head in meter in no leak condition
Y'_1	Inlet pressure head in meter in leak condition
Y'_2	Outlet pressure head in meter in leak condition
Z_1	Datum head in meter at inlet
Z_2	Datum head in meter at outlet
V_1	Inlet velocity in m/s for no leak condition
V_2	Outlet velocity in m/s for no leak condition
V'_1	Inlet velocity in m/s for leak condition
V'_2	Outlet velocity in m/s for leak condition
'f'	Friction factor
'd'	Diameter of pipe in meter
S	Specific pipe resistance given by Darcy-Weisbach frictional loss equation in s2/m6
γ	Specific unit weight of water 9810 N/m^3
'g'	Acceleration due to gravity 9.81 m/s^2
ΔP	Pressure difference between inlet and outlet
'h_f'	Frictional head loss in meter
MS	Mild Steel
PVC	Polyvinyl Chloride
HDPE	High-density Polyethylene

References

Abdulshaheed, A., Mustapha, F., and Anuar, M. (2018). "Pipe material effect on water network leak detection using a pressure residual vector method." *J. Water. Resour. Plann. Manag.*, 144(4). 10.1061/(asce)wr.1943-5452.0000798

Abed, M.H., Wali, W.A., and Alaziz, M. (2023). *Moveable inspection ball simulation for pipe leakage detection using an acoustic sensor*., 10.1109/iiccit55816.2022.10010679

Adedeji, K.B., Hamam, Y., Abe, B.T., and Abu-Mahfouz, A.M. (2017). "Towards achieving a reliable leakage detection and localization algorithm for application in water piping networks: An overview." *IEEE Access*, 5, 20272–20285. 10.1109/ACCESS.2017.2752802

Adegboye, M.A., Fung, W.K., and Karnik, A. (2019a). "Recent advances in pipeline monitoring and oil leakage detection technologies: Principles and approaches." *Sensors (Switz.)*, 19(11). MDPI AG10.3390/s19112548

Adegboye, M.A., Fung, W.K., and Karnik, A. (2019b). "Recent advances in pipeline monitoring and oil leakage detection technologies: Principles and approaches." *Sensors (Switz.)*, 19(11). MDPI AG. 10.3390/s19112548

Adegboye, M.A., Karnik, A., Fung, W.K., and Prabhu, R. (2022). "Pipeline leakage detection and characterisation with adaptive surrogate modelling using particle swarm optimisation." 2022 9th Int. Conf. on Soft Computing and Machine Intelligence, ISCMI 2022, 129–134. https://doi.org/10.1109/ISCMI56532.2022. 10068436

Akinsete, O., and Oshingbesan, A. (2019). "Leak detection in natural gas pipelines using intelligent models." SPE-198738–MS. http://onepetro.org/SPENAIC/proceedings-pdf/19NAIC/2-19NAIC/D023S009R001/1182833/spe-198738-ms.pdf/1

Ali, A.S., Abdelmoez, M.N., Heshmat, M., and Ibrahim, K. (2022). "A solution for water management and leakage detection problems using IoTs based approach." *Internet Things (Neth.)*, 18. 10.1016/j.iot.2022.100504

Ali, S., Hawwa, M.A., and Baroudi, U. (2022b). "Effect of leak geometry on water characteristics inside pipes." *Sustainability (Switz.)*, 14(9), 5224. 10.3390/su14095224

Bakhtawar, B., and Zayed, T. (2021). "Review of water leak detection and localization methods through hydrophone technology." *J. Pipeline Syst. Eng. Pract.*, 12(4). 10.1061/(asce)ps.1949-1204.0000574

Basnet, L., Brill, D., Ranjithan, R., and Mahinthakumar, K. (2023). "Supervised machine learning approaches for leak localization in water distribution systems: Impact of complexities of leak characteristics." *J. Water. Resour. Plann. Manag.*, 149(8). 10.1061/jwrmd5.wreng-6047

Cassa, A.M., van Zyl, J.E., and Laubscher, R.F. (2010). "A numerical investigation into the effect of pressure on holes and cracks in water supply pipes." *Urban Water. J.*, 7(2), 109–120. 10.1080/15730620903447613

Chatzigeorgiou, D.M., Kumar, S., Khalifa, A.E., Deshpande, A., Youcef-Toumi, K., and Sarma, S. (2010). In-pipe Acoustic Characterization of Leak Signals in Plastic Water-filled Pipes AWWA Annual Conference and Exposition (ACE), Chicago.

Cheng, W., Fang, H., Xu, G., and Chen, M. (2018). "Using SCADA to detect and locate bursts in a long-distance water pipeline." *Water. (Switz.)*, 10(12). 10.3390/w101217271727

Chew, A.W.Z., Wu, Z.Y., Kalfarisi, R., Meng, X., and Pok, J. (2023). "Generalized acoustic data analysis framework for leakage detection and localization in Field operational water distribution networks." *J. Water. Resour. Plann. Manag.*, 149(11). 10.1061/jwrmd5.wreng-6122

Colombo, A.F., and Karney, B.W. (2002). "Energy and costs of Leaky Pipes: Toward comprehensive picture." *J. Water. Resour. Plann. Manag.*, 128(6), 441–450. 10.1061/(asce)0733-9496(2002)128:6(441)

De Sousa, C.A., and Romero, O.J. (2017). "Influence of oil leakage in the pressure and flow rate behaviors in pipeline." *Latin Am. J. Energy Res.*, 4(1), 17–29. 10.21712/lajer.2017.v4.n1.p17-29

Du, X., Lambert, M.F., Chen, L., and Jing Hu, E. (2023). "Linking and comparison of the damping of fluid transients and frequency response diagram methods for pipe leak and burst detection and localization." *J. Hydraul. Eng.*, 149(1). 10.1061/jhend8.hyeng-13215

Du, X., Lambert, M.F., Chen, L., Jing Hu, E., and Xi, W. (2020). "Pipe burst detection, localization, and quantification using the transient pressure damping method*J. Hydraul. Eng.*, 146(11). 10.1061/(asce)hy.1943-7900.0001810

Fan, H., Tariq, S., and Zayed, T. (2022). Acoustic leak detection approaches for water pipelines. Automation in construction, Vol. 138. Elsevier B.V. 10.1016/j.autcon.2022.104226

Ferrante, M. (2012). "Experimental investigation of the effects of pipe material on the leak head-discharge relationship." *J. Hydraul. Eng.*, 138(8), 736–74310.1061/(asce)hy.1943-7900.0000578

Fu, Y., and Chen, B. (2024). "Locating blockage and leak in piping systems based on valve stroking." *J. Pipeline Syst. Eng. Pract.*, 15(1), 1–12. 10.1061/jpsea2.pseng-1519

Hadji, A., Flazi, S., and Bouzid, M.A. (2022). "Novel electrical technique for detecting water leaks in buried plastic water distribution pipes." *J. Pipeline Syst. Eng. Pract.*, 13(4). 10.1061/(asce)ps.1949-1204.0000682

Hinderdael, M., Jardon, Z., and Guillaume, P. (2020). An analytical amplitude model for negative pressure waves in gaseous media. Mechanical systems and signal processing, Vol. 144, Elsevier, October, p. 106800.

Jaumouillé, E., Piller, O., and Van Zyl, J.E. (2009). "Advantages of a hydraulic saint-venant type model with pressure-dependent leakage." Proceedings of the 10th Annual Water Distribution Systems Analysis Conference, WDSA 2008, United States, 814–823. https://doi.org/10.1061/41024(340)70

Juliano, T.M., Meegoda, J.N., and Watts, D.J. (2013). "Acoustic emission leak detection on a metal pipeline buried in Sandy Soil." *J. Pipeline Syst. Eng. Pract.*, 4(3), 149–155.10.1061/(asce)ps.1949-1204.0000134

Kammoun, M., Kammoun, A., and Abid, M. (2022). "Leak detection methods in water distribution networks: A comparative survey on artificial intelligence applications." *J. Pipeline Syst. Eng. Pract.*, 13(3), 1–15. 10.1061/(asce)ps.1949-1204.0000646

Kang, D., and Lansey, K. (2014). "Novel approach to detecting pipe bursts in water distribution networks." *J. Water. Resour. Plann. Manag.*, 140(1), 121–127. 10.1061/(asce)wr.1943-5452.0000264

Kocaman, S., Evangelista, S., Guzel, H., Dal, K., Yilmaz, A., and Viccione, G. (2021). "Experimental and numerical investigation of 3D Dam-break Wave propagation in an enclosed Domain with dry and wet bottom." *Appl. Sci.*, 11(12), 5638. 10.3390/app11125638 Open Access

Kousiopoulos, G.P., and Nikolaidis, S. (2022). "Acoustic method for leak size estimation in fluid-carrying pipelines." 2022 11th International Conference on Modern Circuits and Systems Technologies, MOCAST 2022, Univ. of Bremen, Germany, 1, 1–5. https://doi.org/10.1109/MOCAST54814.2022.9837751

Kumar, P., and Mohapatra, P.K. (2022). "Partial blockage detection in pipelines by modified reconstructive method of characteristics technique." *J. Hydraul. Eng.*,148(4), 1–15. 10.1061/(asce)hy.1943-7900.0001971

Li, Z., Wang, J., Yan, H., Li, S., Tao, T., and Xin, K. (2022). "Fast detection and localization of multiple leaks in water distribution network jointly driven by simulation and machine learning." *J. Water. Resour. Plann. Manag.*, 148(9). 10.1061/(asce)wr.1943-5452.0001574

Lin, J., Wang, X., and Ghidaoui, M.S. (2019). "Theoretical investigation of Leak's impact on normal modes of a water–filled pipe: Small to large leak impedance." *J. Hydraul. Eng.*,145(6). 10.1061/(asce)hy.1943-7900.0001606

Lopezlena, R., and Sadovnychiy, S. (2019). "Pipeline leak detection and location using boundary feedback estimation: Case study." *J. Pipeline Syst. Eng. Pract.*, 10(3). 10.1061/(asce)ps.1949-1204.0000382

Pan, B., Keramat, A., and Duan, H.-F. (2023). "Energy analysis for transient-leak interaction and implication to leak detection in water pipeline systems." *J. Hydraul. Eng.*,149(9), 1–12. 10.1061/jhend8.hyeng-13348

Romero-Ben, L., Alves, D., Blesa, J., Cembrano, G., Puig, V., and Duviella, E. (2022). "Leak localization in water distribution networks using Data-driven and model-based approaches." *J. Water. Resour. Plann. Manag.*, 148(5). 10.1061/(asce)wr.1943-5452.0001542

Sophocleous, S., Savić, D., and Kapelan, Z. (2019). "Leak localization in a real water distribution network based on search-space reduction." *J. Water. Resour. Plann. Manag.*, 145(7). 10.1061/(asce)wr.1943-5452.0001079

Steffelbauer, D.B., Deuerlein, J., Gilbert, D., Abraham, E., and Piller, O. (2022). "Pressure-leak duality for leak detection and localization in water distribution systems." *J. Water. Resour. Plann. Manag.*, 148(3). 10.1061/(asce)wr.1943-5452.0001515

Wang, X., Li, J., Liu, S., Yu, X., and Ma, Z. (2022). "Multiple leakage detection and isolation in district metering areas using a multistage approach*J. Water. Resour. Plann. Manag.*, 148(6). 10.1061/(asce)wr.1943-5452.0001558

Zaman, D., Tiwari, M.K., Gupta, A.K., and Sen, D. (2020). A review of leakage detection strategies for pressurised pipeline in steady-state. Engineering failure analysis, Vol. 109, Elsevier Ltd. 10.1016/j.engfailanal.2019.10426

Zeng, W., Gong, J., Cook, P.R., Arkwright, J.W., Simpson, A.R., Cazzolato, B.S., Zecchin, A.C., and Lambert, M.F. (2020). "Leak detection for pipelines using In-pipe optical fiber pressure sensors and a paired-irf technique." *J. Hydraul. Eng.*, 146(10), 1–6. 10.1061/(asce)hy.1943-7900.0001812